Journal of Magnetics 1(2), 94-100 (1996)

A Magnetic Hysteresis Curve Tracer for Rare Earth Ferromagnets

J. R. Rhee

Physics Department, Sookmyung Women's University, Seoul 140-742, Korea

(Received 30 December 1996)

A hysteresis loop tracer using a pulsed high magnetic field of 113.4 kOe, which is suitable for rare earth based permanent magnets, is constructed. The high pulsed magnetic field is generated by discharging a large capacitance charge (5 mF) with a voltage of 600 V into an air solenoid with the inner diameter of 14 mm, outer diameter of 36 mm and the length of 34 mm. A computer simulation method is used for the construction of an electromagnet to optimize the many parameters such as the discharge current, generated pulsed magnetic field intensity, thermal dissipation, capacitance, charged voltage, period of damping oscillation and solenoid geometry. By using the hysteresis loop tracer constructed in this work, we are able to measure hysteresis loops of several rare earth based permanent magnets with large values of the remanent magnetization, coercvity and energy product.

1. Introduction

Much work is currently under way on rare earth permanent magnets (NdFeB and SmCo based magnets) which exhibit large values of remanent magnetization, coercivity and energy product, compared to conventional magnets such as ferrites and AlNiCo [1-6]. With their excellent permanent magnetic properties particularly large coercivity, it is required to apply magnetic fields as large as 50 kOe for a full saturation; in this regard, the measurements of magnetic properties of rare earth based magnets have been a problem in the circles of research community by using conventional electromagnets which normally can generate maximum magnetic fields up to 20 kOe. The magnetic properties of rare earth based permanent magnets are frequently measured by firstly magnetizing the magnets with a pulsed field of about 100 kOe and then applying magnetic fields up to 20 kOe in the direction opposite to the magnetization direction to obtain the demagnetization curves in the second quadrant from which the basic magnetic properties are drawn. A static magetic field of 100 kOe can easily be obtained by using a superconducting magnet. The superconducting magnet, however, is not very suitable for magnetic measurements during which the polarity changes frequently. A pulse method has been used to generate magnetic fields greater than 20 kOe and it involves discharging a large capacitance charge into an air solenoid. The pulse method is a convenient way of producing a dynamic magnetic field suitable for magnetic measurements. So far pulse magnetic fields with mono-polarity, which do not allow to measure the whole hysteresis loop from a single measurement, have been generated [7]. The main aim of the present work is to generate pulse magnetic fields with bi-polarity and measure the whole hysteresis loop of a permanent magnet from a single measurement. The pulsed high magnetic fields with bi-polarity [8] are generated by approaching the damping ratio of current amplitude to 1 when a large capacitance charge is discharged into a solenoid. The generated bi-polar magnetic fields permit to measure minor loops as well as major loops, and also to demagnetize the samples.

2. The Principle and Construction

A. The Basic Construction

A schematic diagram of the apparatus is shown in Fig. 1. The charge generated at high dc source *HV* is stored at bipolar capacitor *C* with high voltage and large capacitance via the current limit resistor *RP* and the charge switch *SW*. The semiconductor switch is closed at this stage. The charge stored at *C* by preset voltage *V* discharges through the air solenoid *L* when *SW* is open and *SC* is closed. This results in large pulsed currents at *L* and *RI* and finally large magnetic fields are generated at *L*. The voltages induced at the sample *S* inside the electromagnet and the pick-up coil *SE* are received by digital transient memories *TRS* and *TRH* and are indicated at an oscilloscope or an *XY* recorder *DP*.

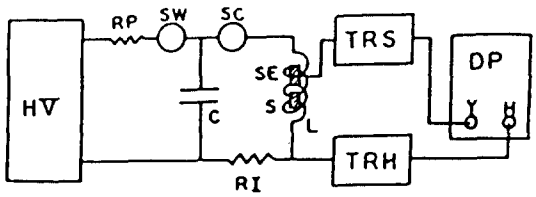

Fig. 1. Block diagram of the pulsed high magnetic field generator.

HV : High Voltage power supply
RP : Protective resistor
S : Sample
SE : Pick up coil for measuring magnetization of sample
SW : Charging Switch
C : Capacitor
SC : Semiconductor Switch
TRS : Transient digital memory for secondary coil
TRH : Transient digital memory for measuring H field
DP : XY display unit

B. The Calculation of Generated Magnetic Field

The following relation (differential equation) holds during the discharge at V;

$$L\frac{d^2i}{dt^2} + R\frac{di}{dt} + \frac{1}{C}i = 0 \tag{1}$$

where L and R, respectively, denote the inductance and the resistance of the air solenoid, and C the capacitance of the capacitor, and i and t are the discharge current and time, respectively. The solution of Eq. (1) is given by;

$$i = \frac{V}{\omega L}\exp\left(-\frac{t}{\tau}\right)\sin\omega t \tag{2}$$

where V is the charged voltage, τ is the time constant of the discharge circuit and is equal to $\tau = 2L/R$, $\omega = (\omega_0^2 - \tau^{-2})^{1/2}$ and $\omega_0 = (LC)^{-1/2}$. The first peak value of i, I_{P1}, is given by;

$$I_{P1} = \frac{V\sin\phi}{\omega L}\exp\left(-\frac{\phi}{\omega\tau}\right) \tag{3}$$

where $\phi = \tan^{-1}\omega\tau$ [9]. The ratio of the second peak value of i, I_{P2}, to I_{P1}, which is denoted by the symbol a, is given by;

$$a = \frac{I_{P2}}{I_{P1}} = \exp\left(-\frac{1}{2\omega\tau}\right). \tag{4}$$

When insulated Cu wire with the diameter D is wound onto an air solenoid with the dimension of inner diameter $2A$, outer diameter $2E$ and the length W, and the wired coil is stacked multiply each layer being separated by an insulating paper with the thickness T, the following relations hold;

$$E = \frac{ND(D+T)}{\eta W} + A, \tag{5}$$

$$Y = \pi N(A+E), \tag{6}$$

$$K = W/[W + 1.29E - 0.39A + 0.64W(E-A)/(E+A)], \tag{7}$$

$$L = [K\pi^2 N^2 (A+E)^2/W]\times 10^{-7}, \tag{8}$$

$$R = 4\rho Y/\pi D^2. \tag{9}$$

Here N is the total number of turns, Y the total coil length, K the coil shape coefficient, R the coil resistance, and η and ρ are the stacking ratio of the Cu wire and the resistivity, respectively. By inserting values given in equations (5)-(9) into equations (1)-(4), the parameters of the electromagnet may be obtained. The maximum magnetic field, B_P, is obtained to

$$B_P = \frac{\mu_0 NI}{2(E-A)}\ln\frac{E+\sqrt{E^2+(W/2)^2}}{A+\sqrt{A^2+(W/2)^2}}, \tag{10}$$

where μ_0 is the permeability in vacuum.

C. The Generation of Bi-polar Pulse Magnetic Field

One of the main tasks of the present work, as was already stated in the Introduction, is to generate bi-polar, pulsed magnetic fields with the amplitude damping ratio close to 1. It is seen from Eq. (4) that the amplitude damping ratio approaches to 1 when the values of ω and τ become very large. The large value of ω is not desiable due to large eddy currents, which produce large values of coercivity and energy product. It is therefore important to minimize the value of ω but to maximize the value of τ, which can be achieved by increasing L and decreasing R and ρ. However the decrease of R is not easy since it depends on the size of coil and furthermore reduces the value of L. In the end, the parameter ρ is the only one which is to be reduced. The value of ρ depends on the type of Cu wire and the temperature. The temperature dependence of ρ is given by;

$$\rho = \rho_0(1+\beta\theta), \tag{11}$$

where ρ_0 is the resistivity at 0 ℃, θ the temperature of coil and β temperature coefficient of resistivity. In the case of Cu wire, $\rho_0 = 1.70\times10^{-8}$ Ωm, $\beta = 4.44\times10^{-3}$/℃ [10]. When the coil is cooled to liquid nitrogen temperature (−196 ℃), ρ is reduced by 11 % compared to room temperature and hence the amplitude damping ratio is expected to increase. The cooling of the coil will also solve the problem of temperature increase of the coil due to Joule heating.

D. Magnetization of Sample and the Measurement of Appied Magnetic Fields

The applied magnetic field H may be measured from Eq. (10) through the measurement of exciting current at the series resistor RI for current measurement. The magnetization M may be obtained by the integration of the induced voltage at the search coil (pick-up coil) which is wound tightly around the sample. The integration can conveniently be done by using an analog integrator.

For the integration circuit with resistor R_s *and capacitor* C_s as shown in Fig. 2, the output voltage V_0 at an analog integrator is given by

$$V_0 = -\frac{1}{R_s C_s} \int v\,dt. \tag{12}$$

The induced voltage at the pick-up coil with Np turns is

$$v = -N_p \frac{d}{dt} [\,\mu_0 Ha_p + \mu_0 x_r Ha_s], \tag{13}$$

where a_p and a_s are cross sectional area of pick-up coil and sample, respectively. The induced voltage at the pick-up coil $-N_p \frac{d}{dt} \mu_0 Ha_P$ is compensated by the voltage induced at the compensation coil which is the same in magnitude but opposite in direction. The magnetization M, therefore, is

$$M = R_s C_s V_0 / N_P a_s. \tag{14}$$

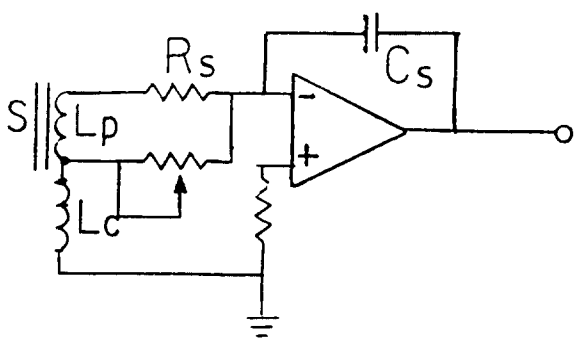

Fig. 2. Integration circuit for measuring magnetization M.
S : Sample, Lp : Pick up coil, Lc : Copensation coil
Rs, Cs : Resistor and Capacitor for integration.

3. Experimental

A. The Design Values of Air Solenoid

The dimension of sample and the design of the solenoid which are able to produce the maximum magnetic field of 100 kG are determined through numerous computer simulations. The details on the sample dimension and the solenoid etc. are given as follows;

sample : cylinder with 6 mm diameter and 5 mm height,
solenoid : $A = 7$ mm, $E = 18$ mm, $N = 300$, $W = 34$ mm,
$T = 0.04$ mm, $D = 1.1$ mm, $\rho = 1.7 \times 10^{-8}$ Ωm,
$C = 0.005$ F, $V = 600$ V, $R = 422$ mΩ, $\tau = 8.7$ ms,
$\omega_0 = 2\pi \times 76.3$ rad/s, $\omega = 2\pi \times 65.8$ rad/s,
$\phi = 1.04$ rad, $I_{PI} = 781$ A, $B_{PI} = 69.7$ kG,
$\alpha = 15.7$ %.

The time dependence of the magnetic field B ($\mu_0 H$) obtained from computer simulation is shown in Fig. 3. The amplitude damping ratio in this case is low (15.7 %) due to large resistivity at room temperature. The parameter values at the liquid nitrogen temperature are given below, except for the parameters independent of temperature.

$R = 52.8$ mΩ, $\tau = 32.9$ ms, $\omega_0 = 2\pi \times 76.3$ rad/s,
$\omega = 2\pi \times 76.18$ rad/s, $\phi = 1.51$ rad, $I_{PI} = 1308$ A,
$B_{PI} = 116.7$ kG, $a = 81.9$ %.

The time dependence of the magnetic field H at the low

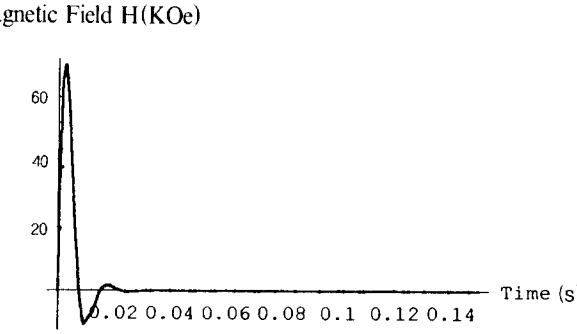

Fig. 3. Time variation of magnetic field H at room temperature.

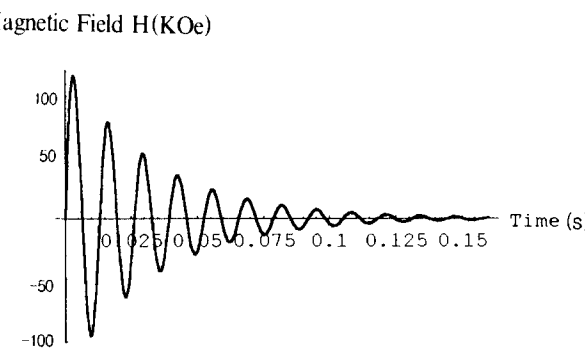

Fig. 4. Time variation of magnetic field H at liquid nitrogen temperature.

temperature is shown in Fig. 4. The amplitude damping ratio in this case is high (81.9 %) due to small resistivity at low temperature. The bipolar pulsed magnetic field B ($\mu_0 H$) achieved at this low temperature is higher than the one at room temperature by 12.0 %.

B. Integration Circuit and Compensation Coil

The lay-out of the compensation coil and the integration cir-

cuit are shown in Fig. 2. Through the use of precision OP amplifier, the stability of the system is found to be very good and the drift very small. Two compensation coils are installed; one at the upper end of the solenoid and the other at the lower end. The number of turns of the coils are adjusted so as to produce zero induced voltage with no sample inserted.

C. The Temperature Control of the Sample

In order to control the sample temperature from the liquid nitrogen temperature to room temperature, 400 turns of Cu wire (with the diameter of 0.06 mm) are wound around the sample case and currents are applied through the wire to generate the Joule heating. The precise control of the temperature are done by the control of the applied voltage and the current through the coil by using a current regulating circuit. In this case the sample temperature is determined by the voltage and the current. Since the sample holder is evacuated to 10^{-3} torr and the thermal conduction is blocked by a suitable design of the holder, the thermal transfer is done only by the radiation. The radiation loss of the sample Pr is determined by the Stephan-Boltzmann law which is given by;

$$\mathrm{Pr} = 5.74 \exp\left[\frac{T_{K1}}{1000} - \frac{T_{K2}}{1000}\right]^4 (\mathrm{W/cm^2}), \qquad (15)$$

where T_{K1} and T_{K2} are the absolute temperatures of the sample and the surrounding (liquid nitrogen), respectively [11].

D. Charging and discharging Circuit.

The charging and discharging circuit is shown in Fig. 5.

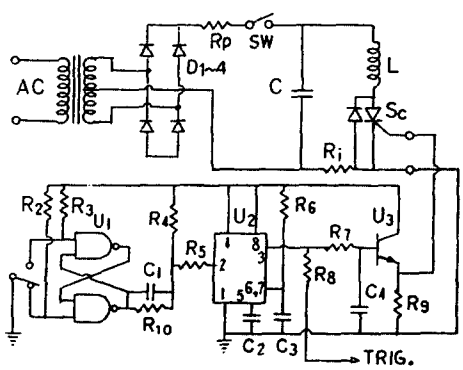

Fig. 5. Charging and discharging circuit.
U_1 : 4011, U_2 : 555, U_3 : 2N2222, Sc : CC11V, C : 1kV, 0.05F,
R_1 : 1m, R_2, R_3 : 330K, R_4, R_5 : 1K, R_6 : 100K,
R_7 : 33, R_8 : 5K, R_9 : 100, R_{10} : 33K, in ohm.
C_1, C_2 : 0.01, C_3, C_4 : 2 in microfarad.

E. Time Dependence of Discharge Current at Room Temperature.

The time dependence of the discharging current at room temperature is shown in Fig. 6. The following values are obtained; $V = 570$ V, $I_{P1} = 700$ A, $I_{P2} = 75$ A, $\omega = 2\pi \times 62.1$ rad/s, $\alpha = 11$ %. These values can be compared with the theoretical values; the peak discharging current I_{P1} is 94.3 % of theoretical value, the amplitude damping ratio reduced by 15.7 % and the angular frequency is 94.3 % of theoretical value ($2\pi \times 65.8$ rad/sec). This disagreement, which is considered to be small, results from negligence of circuit resistance and voltage drop of semiconductor parts in the theoretical calculation.

F. Time Dependence of Discharging Current at Liquid Nitrogen Temperature.

The time dependence of the discharging current at Liquid nitrogen temperature −196 ℃ is shown in Fig. 7 for the charge voltage of 600 V. The following values are obtained; $I_{P1} = 1270$ A, $I_{P2} = 942$ A, $\omega = 2\pi \times 71.3$ rad/s, $\alpha = 74.0$ %. These values can be compared with the theoretical values; I_{P1} is 97.1 % of theoretical value 1308 A, I_{P2} is 88.0 % of theoretical value, the amplitude damping ratio reduced to 90 % of theoretical value (81.9 %) and the angular frequency is 93.6 % of theoretical value ($2\pi \times 76.18$ rad/sec). This disagreement again is considered to be small. The resistance of the temperature sensing coil, R_T, is 15.1 Ω and is 23.4 % of room temperature resistance of 64.5 Ω. This value is larger than that expected from Eq. (11),

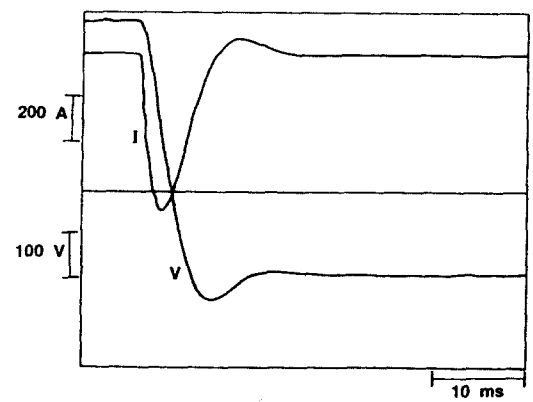

Fig. 6. Time variation of discharging current I and voltage V at room temperature (measured).

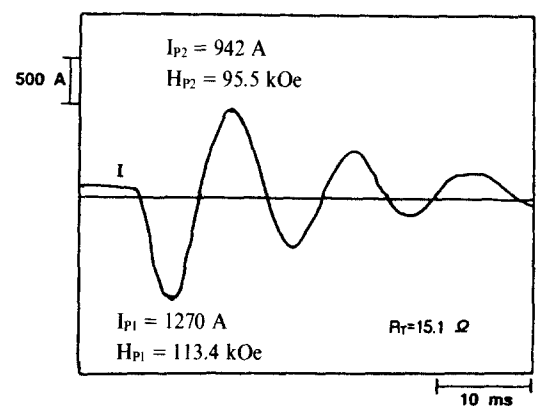

Fig. 7. Time variation of discharging current I at −196 ℃ (measured). R_T : Resistance of coil for measuring temperature.

since it is considered that the resistance temperature coefficient β is different from the value reported in the literature (4.44×10^{-3}/℃) and the slope of the linearity is reduced at low temperatures. If it is assumed that Eq. (11) holds, β is calculated to be 3.56×10^{-3}/℃ by using the experimental R_T and this value is in agreement with theoretical expansion coefficient of ideal gas (1/273). It is determined from Eq. (10) that the magnetic field H_{P1} is 113.4 kOe at I_{P1} = 1270 A and H_{P2} is 95.5 kOe at I_{P2} = 942 A.

G. Calibration of Magnetization with Ni Standard Sample

The calibration of the hysteresis loop tracer constructed in this work is carried out by using a standard Ni sample (cylinder with 5 mm diameter and 5mm height) with the purity of 99.9 %. The results for the variation of current I and the output voltage at the integrator V_0 with time are obtained when the resistance of the temperature measurement coil reaches 23 Ω which normally takes 90 minutes after introducing liquid nitrogen and the results are shown in Fig. 8. At this time, I_{P1} = 74.7 A and I_{P2} = 53 A and the corresponding applied peak magnetic fields are; H_{P1} = 6.67 kOe and H_{P2} = 4.73 kOe.

The output voltage at the integrator which is proportional to magnetization M is 142.8 mV at saturation. Then M_s can be

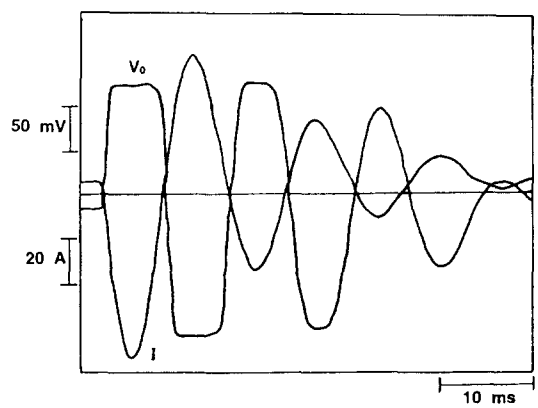

Fig. 8. Out put voltage V_0 of the integrator and discharging current I as a function of time t at −196 ℃. Sample : Pure Ni rod (5 mm in diameter and 5 mm long).

obtained from Eq. (14) and it is calculated to be 6.06 kG with the values of R_s = 10 kΩ, C = 0.2 μF, N_P = 24, $a_s = \pi \times 2.5^2 \times 10^{-6}$ m^2. The M_s value of 6.06 kG obtained from the loop tracer constructed in this work is in good agreement with those reported in the literature; 6.04 kG at −273 ℃ and 6.08 kG at 20 ℃ [12]. At room temperature, a voltage of 5.7 V is applied to the temperature control coil and the resulting current at the coil is 0.087 A which is measured 90 minutes after applying the voltage. This indicates that the value of R_T is 65.5 Ω which is larger than the value of 64.5 at 20 ℃. The temperature of the sample therefore is calculated to be 24.4 ℃ using the experimentally obtained temperature coefficient of the resistance (0.00356). The output voltage at the integrator is 138.6 mV according to the results shown in Fig. 9. This results in the M_s value of 5.9 kG which is smaller than that reported in the literature [11] by 3.5 %. One of the reasons behind the discrepancy is the difference in the measured temperatures; the value is obtained at 24.4 ℃ while the reported one at 20 ℃.

In Fig. 10 are shown the results for M-H curves, which are obtained from the results shown in Fig. 9 for the H-t and M-t curves. Both major and minor loop are obtained simultaneously. The value of coercive force is 614 G at H_{P1} = 6.67 kOe and it decreases with decreasing applied field. This is considered to be due to the eddy currents induced during the ac measurements.

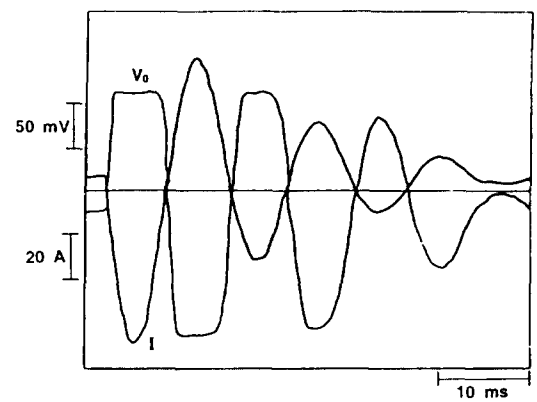

Fig. 9. Out put voltage V_0 of the integrator and discharging current I as a function of time t at 24.4 ℃. Sample : Pure Ni rod (5 mm in diameter and 5 mm long).

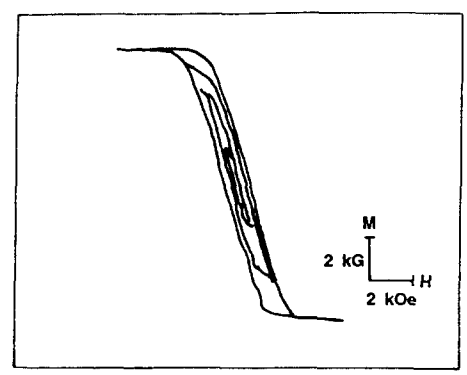

Fig. 10. Magnetic hysteresis curves of pure Ni rod. (replotted from Fig. 9.)

H. Hysteresis Loops of NdFeB Magnets

In Fig. 11(a) are shown the results for the variation of M with time at several applied fields for NdFeB magnets (supplied from Daewoo heavy industry) with the dimension of 6 mm diameter and 5 mm height. The measured temperature is 10 ℃. The first peak value of applied field, H_{P1}, is 113.4 kOe and the second one, H_{P2}, is 86.4 kOe. The difference in the first and second peak values of M is 952 mV measured at the integrator and the peak to peak value of M is calculated to be 28.2 kG from Eq. (14). Also the difference in the second and third peak

values of M is 867 mV and the value of M is 12.8 kG. The value of M_s is therefore 14.1 kG which is the half of the peak to peak value. Also the difference in the second and third peak values of M is 867 mV and the value of M_s is 12.8 kG. In Fig. 11(b) the value of coercive force is 20.0 kOe measured at the first and second peak values and it is 13.3 kOe at the second and third peak values. Similar results at the temperature of −149 ℃ are shown in Fig. 12(a). The applied magnetic fields are the same as in Fig. 11(a). The value of M_s measured from the first and second peaks is 14.1 kG which is equal to that measured at 10 ℃ but the value of M_s measured from the second and third peaks is 13.5 kG which is larger than the value measured at 10 ℃ by 5.2 %. In Fig. 12(b) the value of coercive force is increased significantly; the value of 37.3 kOe is obtained from the first and second peak values. This may indicate that the magnetic anisotropy is very large at low temperatures. Although a detailed comparison with other reported results is not made in this work due to unavailability of the composition of the magnet supplied from Daewoo heavy industry, it is considered that the present results are in line with the reported ones.

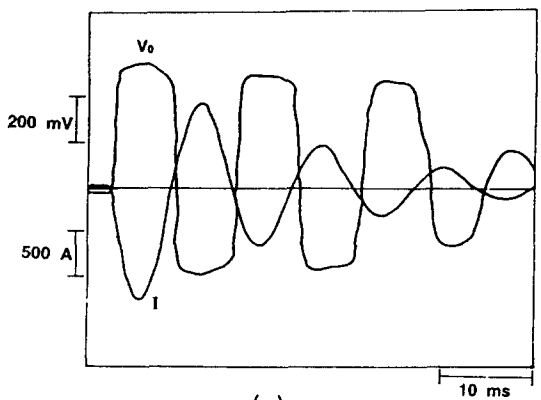

(a)

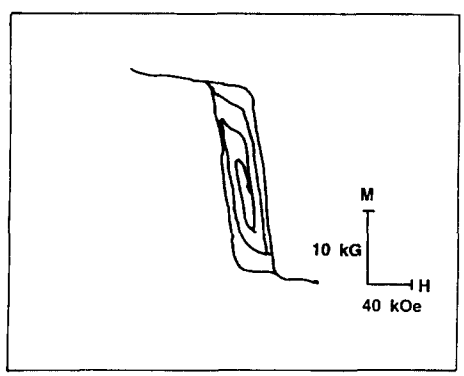

(b)

Fig. 11. Magnetization and applied field for a NdFeB magnet as a function of time t at 10 ℃ (left) and hysteresis curves (right). (R_T = 61.5 Ω)

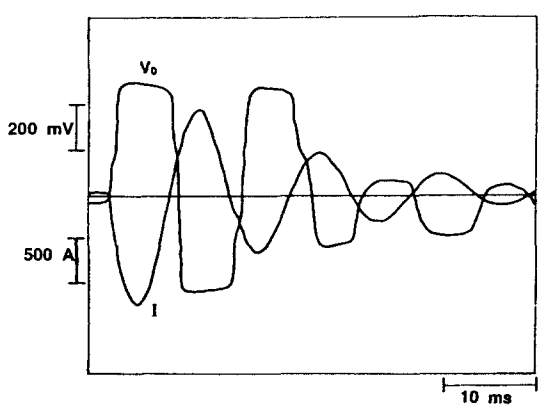

(a)

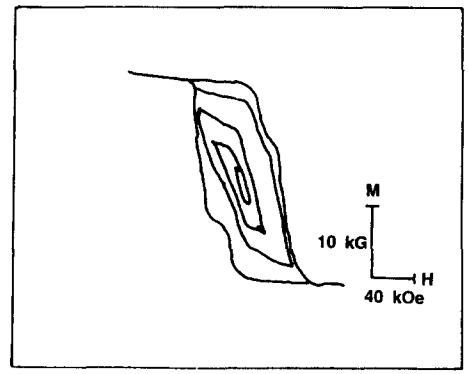

(b)

Fig. 12. Magnetization and applied field for a NdFeB magnet as a function of time t at −149 ℃ (left) and hysteresis curves (right). (R_T = 24.5 Ω)

4. Conclusions

The present results are summarized as follows;

1. A charge stored at a capacitor with 0.005 F and 600 V is discharged to an air solenoid (14 mm inner diameter, 36 mm outer diameter and 34 mm length) which is maintained at the liquid nitrogen temperature of −196 ℃ and the following values are obtained; the maximum magnetic field of 113.4 kOe, the amplitude damping ratio of 74 % and the angular frequency of $2\pi \times 71.3$ rad/sec. These results are in agreement, within 90 %, with the theoretical ones which are obtained by neglecting circuit resistance and voltage drop of semiconductor parts.
2. By using the ac magnetic fields generated in 1, the appratus is calibrated with Ni standard samples and the hysteresis loops of NdFeB magnets are obtained. The results obtained in the present work are found to be reasonable.
3. The value of coercive force of NdFeB magnets are measured to be very large at low temperatures indicating a large value of magnetic anisotropy at low temperatures.

References

[1] B. M. Ma, C. O. Bounds et al "Comparison of the im-

provement of thermal stability of NdFeB sintered Magnets" J. Appl. Phys., **75**, 6628 (1993).

[2] Raja K. Mishra, V. Panchanathan, "Microstructure of high remanance NdFeB alloys with low rare-earth content" J. Appl. Phys., **75**, 6652 (1993).

[3] H. H. Stadelmaire "Intermetallics for permanent magnets" IEEE, Trans. MAG-29, 2741 (1993).

[4] M. Sagawa and H. Nagata, "Novel processing technology for permanent magnets" IEEE, Trans. MAG-29, 2747 (1993).

[5] Y. Nakagawa and H. Kato "Magnetic Hysteresis and Demagnetizing -Field Correction for Rare Earth Magnets", J. Magn. Soc. Japan. **18**, 221 (1994).

[6] K. Ikuma and H. Miyadera, "High Energy Extrusion Molded NdFeB Magnets" J. Magn. Soc. Japan, **18**, 221 (1994).

[7] T. Nishio, Y. Iwama, Solid state physics **15** (3) pp. 165 ~ 170 (1980).

[8] J. R. Rhee and Y. H. Lee, to be published.

[9] S. Chikazumi, Magnetism. pp 123 ~ 161 (Kyoritsu Pub. Co., Tokyo) (1977).

[10] M. Iyeda et al, Electric and Electronic Handbook, pp. 594 ~ 597, Tomokura Co, Tokyo, (1988).

[11] J. Yoshimura "Design and Calibration of Radio Frequency Furnace" p 18, Seibundo Co, Tokyo (1966).

[12] "Technical manual of Metaglass magnetic materials", (Japan Armorphous Metals Co, Tokyo, 1980).